BAL is a novel risk-related gene in diffuse large B-cell lymphomas that enhances cellular migration

Ricardo C. T. Aguiar, Yoshihiro Yakushijin, Samir Kharbanda, Ravi Salgia, Jonathan A. Fletcher, and Margaret A. Shipp

Clinical risk factor models such as the International Prognostic Index are used to identify diffuse large B-cell lymphoma (DLB-CL) patients with different risks of death from their diseases. To elucidate the molecular bases for these observed clinical differences in outcome, differential display was used to identify a novel gene, termed *BAL* (B-aggressive lymphoma), which is expressed at significantly higher levels in fatal high-risk DLB-CLs than in cured low-risk tumors. The major *BAL* complementary DNA encodes a previously uncharacterized 88-kd nuclear protein with a duplicated N-terminal domain homologous to the non-histone portion of histone-macroH2A and a C-terminal alpha-helical region with 2 short coiled-coil domains. Of note, the BAL N-terminus and secondary structure resemble those of a recently identified human protein, KIAA1268. In addition, both *BAL* and *KIAA1268* map to chromosome 3q21, further suggesting that these genes belong to a newly identified family. BAL is expressed at increased levels in DLB-CL cell lines with an activated peripheral B cell, rather than a germinal center B cell, phenotype. This observation and the characteristic dissemination of high risk DLB-CLs prompted studies regarding the role of BAL in B-cell migration. In classical transwell assays, stable BAL-overexpressing B-cell lymphoma transfectants had significantly higher rates of migration than vector-only transfectants, indicating that the risk-related *BAL* gene promotes malignant B-cell migration. (Blood. 2000;96:4328-4334)

Introduction

Diffuse large B-cell lymphoma (DLB-CL) is a clinically heterogeneous disorder and the most common lymphoid malignancy in adults.[1] Although approximately 40% of DLB-CL patients can be cured with standard therapy, the majority will ultimately die of their disease.[1]

Prognostic models based on pretreatment clinical characteristics can be used to identify DLB-CL patients with different risks of death from their diseases. The International Prognostic Index (IPI) is a widely accepted clinical risk factor model that delineates DLB-CL patients with low (L)-, low-intermediate (LI)–, high-intermediate (HI)–, and high (H)-risk disease and associated differences in overall survival.[2] Although the IPI is a useful clinical tool for assessing prognosis and individualizing therapy, the model is based on imprecise clinical features (eg, age, stage of disease, number of extranodal sites, serum lactate dehydrogenase (LDH), and performance status).[2] Clearly, these clinical features are surrogate variables for intrinsic cellular and molecular heterogeneity in DLB-CL. For example, the mechanisms responsible for the widespread dissemination and extranodal involvement of high-risk DLB-CLs are not yet known.

The extent to which malignant B-cell migration recapitulates that of its normal counterparts remains to be defined.[3,4] The putative normal counterparts of DLB-CLs are mature B cells that have migrated to secondary lymphoid organs, encountered antigens, engaged their B-cell receptors, and subsequently moved to the germinal center (GC) where they undergo hypermutation and affinity maturation.[3,5,6] A subset of DLB-CLs is thought to be derived from mature effector cells that have exited the GC and re-entered the circulation.[3,7] The events that govern the migration of normal antigen-activated B cells and their malignant counterparts are the subject of intense investigation.[4-6,8-10]

As part of an effort to identify genes associated with the unique behavior of curable L/LI-risk and fatal HI/H-risk DLB-CLs, we have isolated and characterized a novel risk-related gene, termed *BAL* (B-aggressive lymphoma), which promotes malignant B-cell migration.

Materials and methods

Cell lines and primary tumor specimens

Human DLB-CL cell lines DHL-4, DHL-6, DHL-7, DHL-8, DHL-10, and the aggressive B-cell lymphoma cell line Namalwa, were cultured in RPMI 1640 supplemented with 10% heat-inactivated fetal calf serum, 2 mmol/L glutamine, 1 mmol/L sodium pyruvate, and 10 mmol/L Hepes buffer and penicillin/streptomycin.[11] The human DLB-CL cell lines OCI-Ly3 and OCI-Ly10 were cultured in Iscove modified Dulbecco medium (IMDM) containing 20% fresh human plasma. Cryopreserved primary tumor specimens were obtained from DLB-CL patients with known clinical characteristics, well-defined IPI risk profiles and long-term follow-up. Total RNA was isolated from the cell lines and primary tumors as previously described.[11]

From the Department of Adult Oncology, Dana-Farber Cancer Institute, and the Department of Pathology, Brigham and Women's Hospital, Harvard Medical School, Boston, MA.

Reprints: Margaret A. Shipp, Dana-Farber Cancer Institute, 44 Binney St, Boston, MA 02115; e-mail: margaret_shipp@dfci.harvard.edu.

Submitted June 14, 2000; accepted September 26, 2000.

Supported by National Institutes of Health (NIH) grant CA66996 and a Larry and Susan Marx Research Fellowship (R.C.T.A.). R.C.T.A. is currently a Special Fellow; M.A.S. is a Scholar of the Leukemia and Lymphoma Society of America.

The publication costs of this article were defrayed in part by page charge payment. Therefore, and solely to indicate this fact, this article is hereby marked "advertisement" in accordance with 18 U.S.C. section 1734.

Differential display, cDNA cloning, and sequencing

Differential display was performed as previously described.[11,12] The relevant differential display product was used as a probe to screen a size-selected anti–Ig-activated normal B-cell cDNA library (a gift from G. Freeman, Boston, MA). *BAL* full-length cloning was completed with 5′ and 3′ rapid amplification of cDNA ends (RACE) polymerase chain reaction (PCR), performed as previously described.[11] All DNA sequencing was performed on an Applied Biosystems model 373A automated sequencer (Perkin-Elmer, Norwalk, CT).

Northern blot analysis

Total RNA from DLB-CL cell lines and primary tumors was isolated, size-fractionated in 1% agarose/formaldehyde gels and transferred to nylon membranes as described.[11] These membranes and additional multiple tissue northern blots (Clontech, Palo Alto, CA) were hybridized according to standard protocols with either the reamplified *BAL* differential display fragment, an additional approximately 800-bp *BAL* cDNA probe, or a probe derived from β-actin.

P1 artificial chromosome library screening, fluorescence in situ hybridization, and somatic cell hybrid mapping

The human P1 artificial chromosome (PAC) library RPCI1 (UK Human Genome Mapping Project [HGMP] Resource Centre, Cambridge, United Kingdom) was screened with a *BAL* cDNA probe according to standard protocols. DNA from positive clones was southern-blotted and rehybridized with a second unique *BAL* probe to confirm specificity. PAC DNAs were labeled with biotin and hybridized to human normal metaphases as previously described.[13] Image analyses were performed with a cooled CCD camera (Photometrics, Roper Scientific, Trenton, NJ) in conjunction with an image analysis system (Oncor; Ventana Medical Systems, Tucson, AZ). A human monochromosomal somatic cell hybrid DNA panel (UK HGMP Resource Centre) was also screened by PCR according to the supplier's instructions.

Semi-quantitative duplex reverse transcriptase–polymerase chain reaction

cDNAs were synthesized from primary DLB-CLs from patients with well-defined IPI clinical risk profiles and long-term follow-up as previously described.[14] To control the quantity and quality of input cDNA and the amplification efficiency in individual test tubes, *BAL* cDNA was coamplified with the constitutively expressed *ABL* gene. Duplex reverse transcriptase–polymerase chain reaction (RT-PCR) products were electrophoresed in 2% agarose gels, blotted, and hybridized to internal *BAL* and *ABL* oligonucleotide probes. The abundance of *BAL* in a given sample was determined by comparing the intensity of the coamplified *BAL* and *ABL* PCR products with scanning densitometry. The sensitivity of the duplex RT-PCR was determined by constructing and analyzing a standard dilutional curve (data not shown). In brief, fixed amounts of *BAL*-negative and *BAL*-positive cell line cDNAs were added together to mimic *BAL* losses of 10%-100% and these mixed cDNAs were coamplified for *BAL* and *ABL*. The ratio of the intensity of the *BAL* and *ABL* bands plotted against the percentage of *BAL* "loss" yielded a straight line and an r^2 value of .98, indicating that the assay accurately detects *BAL* expression in primary tumor samples. Oligonucleotide sequences (derived from different exons to avoid amplification of contaminating genomic DNA) and PCR conditions are available upon request.

BAL antibody production

A BAL (aa 592-854)-GST fusion protein was generated using the pGEX-5X-3 expression system (Pharmacia, Piscataway, NJ). The BL21 (DE3) *Escherichia coli* strain (Stratagene, La Jolla, CA) was transfected with the construct and the GST-BAL fusion protein was expressed and purified according to the manufacturer's protocols. BAL-GST antiserum was generated in New Zealand white rabbits via repetitive immunization. The resulting antiserum was depleted of anti-GST antibodies and purified with protein A prior to use.

Transfections, Western blot, and fluorescence microscopy

The full-length BAL_S cDNA was cloned into the green fluorescent protein (GFP) expression vector pEGFP-C (Clontech), the HA-tagged (hemagglutinin protein) pHM6 vector (Boehringer-Mannheim, Mannheim, Germany), and the untagged pRcCMV expression vector (Invitrogen, Carlsbad, CA). Linearized DNAs from all 3 constructs and vectors-only were transfected by electroporation into an aggressive B-lymphoma cell line (Namalwa) and selected with G418 (Sigma, St Louis, MO). The G418-resistant GFP-BAL or GFP-only transfectants were sorted by flow cytometry to select high GFP- or GFP-BAL–expressing cells. The HA-tagged BAL, pRcCMV-BAL, or vector-only transfectants were cloned by limiting dilution as previously described.[11]

Total cell lysates were obtained from DLB-CL cell lines and all tagged (GFP and HA) or untagged (pRcCMV) BAL and vector-only transfectants. Cytoplasmic and nuclear fractions from multiple GFP-BAL_S, HA-BAL, or vector-only transfectants were also isolated[15] and western blots performed as described.[11] Rabbit polyclonal GFP antiserum (Clontech) was used for immunologic detection of GFP-BAL fusion proteins. Murine monoclonal anti-Rb (gift from W. Sellers, Dana-Farber Cancer Institute, Boston, MA) and anti-αtubulin (gift from P. Dahia, Dana-Farber Cancer Institute) were used to assess the purity and loading of the subcellular fractions. A rabbit polyclonal BAL antiserum was used to detect BAL expression in the DLB-CL cell lines and untagged (pRcCMV) BAL and vector-only B-cell lymphoma transfectants.

Murine fibroblast NIH 3T3 cells were seeded on glass coverslips and transfected with GFP-BAL or GFP-only constructs with Superfect (Qiagen, Valencia, CA) according to manufacturer's instructions. Forty-eight hours after transfection, the slides were rinsed with ice-cold phosphate-buffered saline and cells were fixed with 3% paraformaldehyde and analyzed by fluorescence microscopy.

Cell migration assays

Multiple pRcCMV-BAL or vector-only stable B-cell lymphoma transfectants were seeded overnight at 1×10^6 cells/mL in RPMI 10% fetal bovine serum. Thereafter, 2×10^6 cells/mL of each cell type was starved in serum-free AIM-V medium (Gibco-BRL, Gaithersburg, MD) for 1 hour at 37°C in 5% CO^2. Migration assays were subsequently performed using Transwell chambers with 8-μm pore filters (6.5 mm Transwell, polycarbonate membrane; Costar, Cambridge, MA).[16] Cell suspensions (2×10^5 in 100 μL) were added to the upper chambers and 600 μL of medium either containing or lacking recombinant human stromal-derived factor 1 α (SDF-1α) (100 ng/mL; R&D Systems, Minneapolis, MN) was added to each of the lower chambers. After transwells were incubated for 2-4 hours at 37°C in 5% CO2, the cells in each lower chamber were recovered and counted (Coulter particle and size analyzer [Z-2]; Coulter, Hialeah, FL). In each assay, all clones were analyzed in duplicate in the presence or absence of SDF-1α; the entire assay was repeated 3 times.

Results

Identification and cloning of the risk-related *BAL* gene

In initial differential display analyses of primary DLB-CLs from patients with known clinical characteristics, well-defined IPI risk profiles and mature follow-up, we identified a cDNA that was more abundant in tumors from patients with fatal high-intermediate/high–risk (HI/H [IPI]) disease than in tumors from patients with cured low/low-intermediate–risk (L/LI [IPI]) lymphoma. The differential display product was isolated, amplified, and used as a probe in confirmatory northern blot analyses of the same set of DLB-CLs used for the initial differential display experiments. The probe hybridized with an approximately 3.2-kb transcript that was more abundant in HI/H-risk DLB-CLs

than in the L/LI-risk lymphomas (Figure 1A). A full-length cDNA was cloned from an anti–Ig-activated splenic B-cell library and termed *BAL*. Two *BAL* cDNAs were identified (GenBank accession AF307338 and AF307339): a major form of 3105 bp (BAL_S) and a minor alternatively spliced form of 3230 bp (BAL_L).

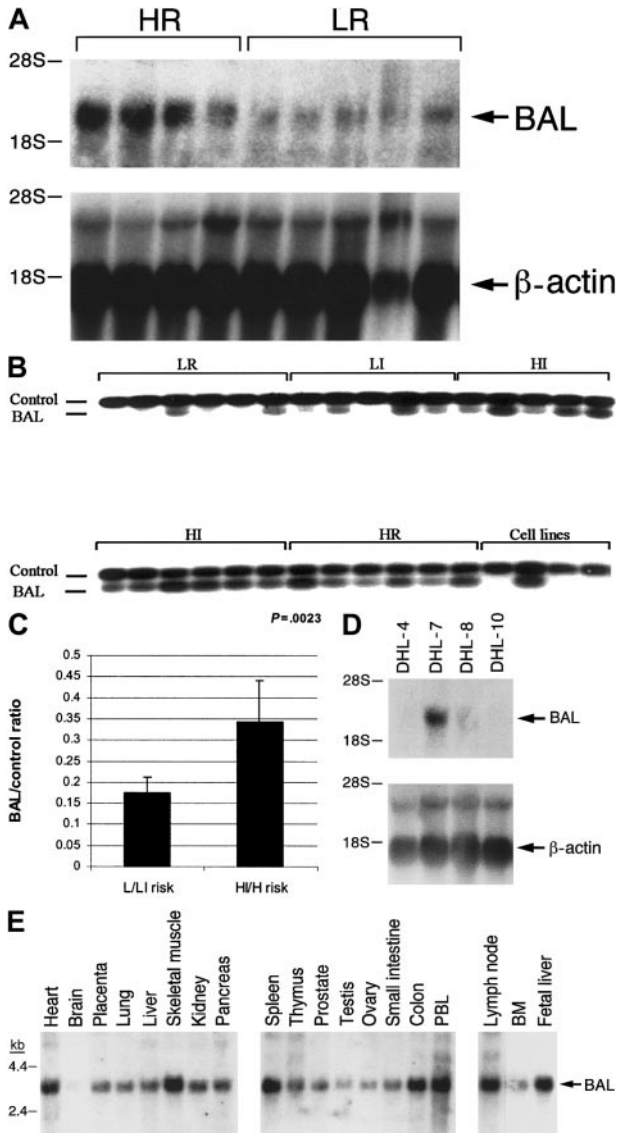

Figure 1. *BAL* expression in DLB-CLs (primary tumors and cell lines) and normal human tissues. (A) Northern blot analysis of primary DLB-CLs from patients with known clinical characteristics, well-defined IPI risk profiles, and mature follow-up whose specimens were analyzed in initial differential display. The filter was hybridized with the differential display product equivalent to the 3′ end of *BAL* cDNA. The approximately 3.2-kb BAL transcript is more abundant in high risk (HR) than in low risk (LR) primary DLB-CLs. The filters were also hybridized with β-actin to confirm equal loading. (B) Semiquantitative duplex RT-PCR analysis of *BAL* expression in an additional series of primary DLB-CLs from patients with well-characterized IPI risk profiles, long-term follow-up, and aggressive B-cell lymphoma cell lines (DHL-4, DHL-7, DHL-8, and DHL-10). (C) Densitometric analysis of *BAL* expression in the expanded series of primary DLB-CLs (shown in B). The abundance of BAL in a given sample was determined by comparing the intensity of coamplified BAL and internal control signals via scanning densitometry. Thereafter, a ratio of the intensity of the 2 bands was generated to reflect BAL expression. Densitometric profiles of BAL expression in tumors from patients with low/low-intermediate–risk and high-intermediate/high–risk (IPI) disease are shown and demonstrated to be significantly different ($P = .0023$, 1-sided Student t test). (D) Northern blot analysis of *BAL* transcripts in the aggressive B-cell lymphoma cell lines (DHL-4, DHL-7, DHL-8, and DHL-10). The filters were also hybridized with β-actin to confirm equal loading. (E) Northern blot analysis of *BAL* transcripts in multiple normal human tissues.

BAL expression in an expanded series of primary DLB-CLs and additional normal human tissues

The risk-related expression of *BAL* in DLB-CLs was further evaluated using a semi-quantitative duplex RT-PCR assay in a larger series of 28 primary DLB-CLs from patients with well-characterized IPI risk profiles and long-term follow-up (Figure 1B-C). This expanded analysis confirmed that *BAL* transcripts were significantly more abundant in HI/H-risk than in L/LI-risk lymphomas ($P = .0023$) (Figures 1B-C).

To assess the possibility that increased BAL expression was simply a reflection of the rapid growth rate of HI/H risk DLB-CLs, 4 aggressive B-cell lymphoma cell lines with high growth rates were also evaluated for *BAL* transcripts. As indicated in Figure 1B,D, 3 of the 4 rapidly proliferating aggressive B-cell lymphoma cell lines expressed low levels of *BAL*, whereas 1 cell line (DHL-7) had more abundant *BAL* transcripts.

BAL transcripts were also readily detectable in normal lymphocyte-rich tissues and specimens such as spleen, lymph nodes, peripheral blood lymphocytes and colonic mucosa, and additional nonhematopoietic organs, particularly heart and skeletal muscle (Figure 1E).

Analysis of the BAL aa sequence and chromosome localization

The major and minor *BAL* cDNAs encode 819aa and 854aa BAL proteins (Figure 2A). The *BAL* N-terminal region contains a duplicated domain of unknown function (http://pfam.wustl.edu) (BAL aa 160-288 and aa 319-485) found in the nonhistone region of histone macroH2A (Figure 2B)[17] and in the nonstructural polyproteins of several RNA viruses.[18] This domain also exists as a whole protein in several bacterial species underscoring the evolutionary conservation and potential functional significance of the region.[18]

Further analysis of BAL's putative secondary structure (www.ibcp.fr [NPS server] and www.ch.embnet.org/software/COILS_form.html) predicts a C-terminal alpha-helical region that includes 2 putative short coiled-coil domains (aa 586-617 and 746-758) (Figures 2B and C). In a coiled-coil, the alpha-helical bundle is wound into a superhelix, with distinctive packing of amino acid sidechains derived from 7 structural positions into a heptad repeat.[19] The putative BAL coiled-coil regions contain 4-heptad (aa 586-617) and 2-heptad (aa 746-758) repeats.[19] The distal BAL C-terminus also contains a single proline-rich sequence with the characteristics of an SH3-binding site, a potential protein-protein interaction domain.[20]

BAL also displays extended partial homology with a recently described partial human cDNA, *KIAA1268*[21] (BAL aa 85-487, 31% identity and 50% homology and BAL aa 160-616, 25% identity and 46% homology, Figure 2C). Whereas BAL contains a duplicated N-terminal domain homologous to the nonhistone region of histone macroH2A, the KIAA1268 N-terminus contains 3 repeats of this region (Figures 2C-D).[17] The KIAA1268 C-terminus is also predicted to include an unrelated alpha-helical region with 2 short coiled-coils (Figure 2C).

The *BAL* locus was mapped to chromosome band 3q21 using fluorescence in situ hybridization (FISH) and analysis of a somatic cell hybrid panel (Figure 3 and data not shown). A group of expressed sequence tags (ESTs) from KIAA1268 are included in the UniGene cluster Hs 152925 (www.ncbi.nlm.nih.gov/UniGene/index.html), which is assigned to a region located between markers D3S3576 and D3S1267 (140-141 cM from the top of the chromosome 3 group) that also coincides with chromosome band 3q21.

By searching the sequence-tagged sites (STS)–based map of the human genome generated by Genethon (www.genethon.fr)

and the Whitehead Institute (www.genome.wi.mit.edu), markers D3S3576 and D3S1267 were anchored to 2 yeast artificial chromosome (YAC) contigs, WC3.16 and WC-329. For these reasons, a series of YACs from these 2 contigs were southern-blotted and hybridized with BAL and KIAA1268 probes (data not shown). Both BAL and KIAA1268 mapped to YAC 822a12, indicating that these 2 genes are located within a small distance ($<$ 1.6 Mb) of each other. Taken together, these data strongly suggest that BAL and KIAA1268 belong to a unique gene family with a variable number of highly conserved N-terminal repeats (http://pfam.wustl.edu) (Figure 2D) and divergent C-terminal alpha-helical domains (Figure 2C) which may have arisen as a consequence of gene duplication in the 3q21 region.[22,23]

Subcellular localization of the BAL protein

To gain additional insights into the predicted BAL structural motifs, we determined the subcellular location of the major BAL protein by transiently transfecting NIH 3T3 cells with a GFP-BAL_S construct and analyzing the fusion protein by fluorescence microscopy. As indicated in Figure 4A, GFP-BAL was primarily located in the nucleus. To confirm that BAL also localized to the nucleus in B-lymphocytes, we transfected GFP-BAL and vector-only GFP constructs into a B-lymphoma cell line with low levels of endogenous BAL and performed subcellular fractionation. The resulting cytoplasmic and nuclear cell fractions were blotted and probed with an anti-GFP antibody (Figure 4B, left panel) or control antibodies directed against known cytoplasmic (αtubulin; Figure 4B, right lower panel) and nuclear (retinoblastoma [Rb], Figure 4B, right upper panel) proteins. In these B-cell transfectants, GFP alone (approximately 26 kd) was primarily detected in the cytoplasm whereas GFP-BAL (approximately 114 kd) was predominantly found in the nucleus (Figure 4B). In an additional series of B-cells transfected with HA-tagged BAL or vector alone, BAL-HA primarily localized to the nucleus (data not shown), indicating that the GFP moiety in the GFP-BAL fusion protein did not alter the protein's subcellular localization.

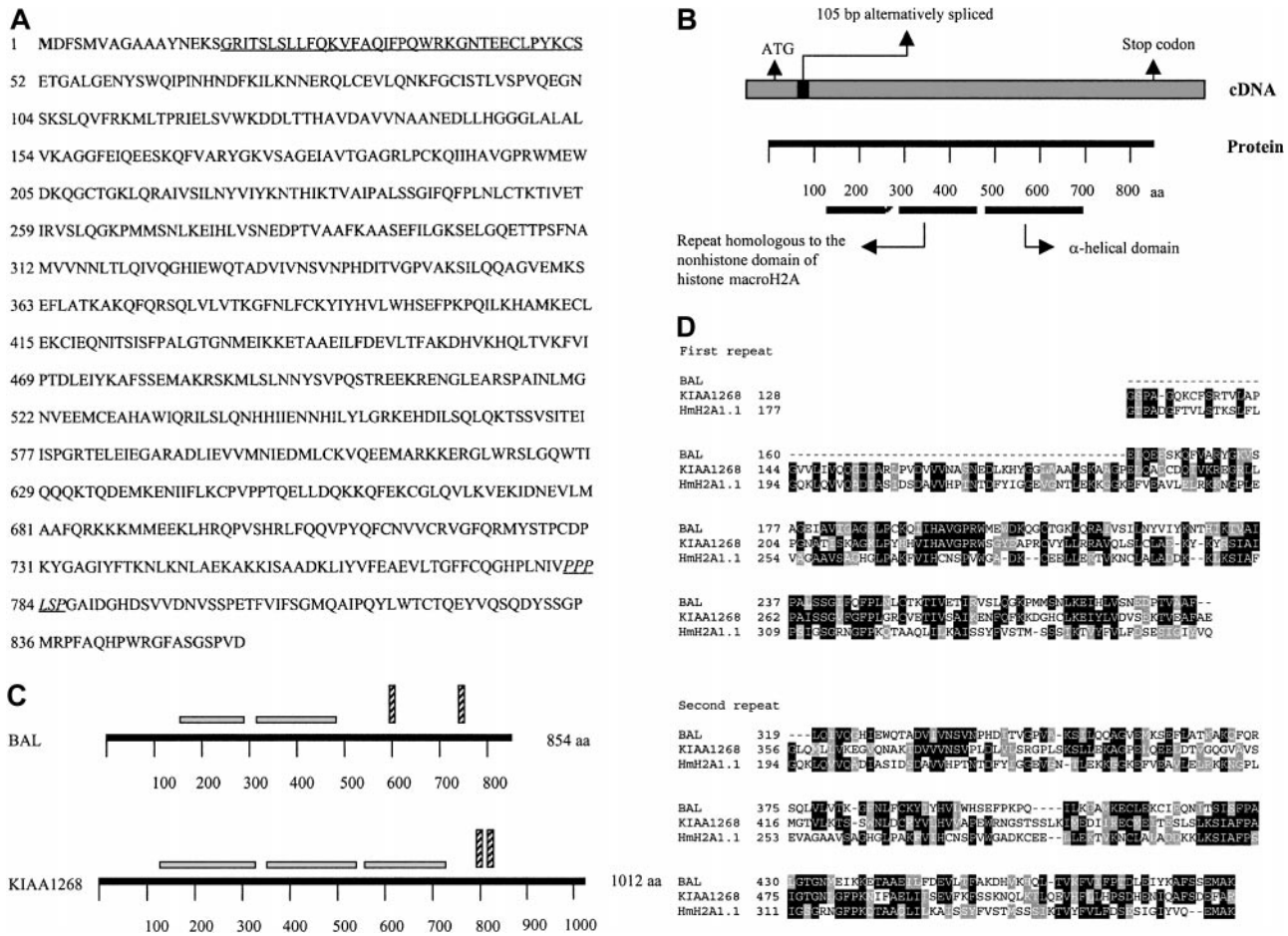

Figure 2. BAL predicted aa sequence and homologies to additional proteins. (A) BAL predicted aa sequence. The predicted initiation methionine, which is bolded, is surrounded by a classic Kozak consensus sequence. The BAL aa sequence (aa 17-51), which is included in the minor ($BAL_{Long(L)}$) form and is spliced out of the major (BAL_S) form, is underlined. A single proline-rich putative SH_3 binding site is also indicated (aa 781-786). (B) Schematic representation of *BAL* cDNA and aa sequence. The BAL N-terminal region contains a duplicated domain of unknown function(http://pfam.wustl.edu; BAL aa 160-288 [22% identity, 42% homology, PSI-BLAST] and aa 319-485 [26% identity, 48% homology, PSI-BLAST]) which is found in the nonhistone region of histone macroH2A.[17] Secondary structure analysis of the proximal C-terminal region of BAL predicts an alpha-helical region. The distal BAL C-terminus also has limited partial homology with the C-terminal region of the recently described TRF-1 interacting ankrin repeat ADP-ribose polymerase (Tankyrase)[33] and a related hypothetical protein, AL 080156 (BAL aa 667-820, 27% identity, 48% homology [with AL080156], PSI-BLAST). Although the Tankyrase C-terminus encodes a poly ADP-ribose polymerase (PARP) domain, several amino acid residues required for PARP activity[33] are not conserved in the BAL C-terminal sequence and BAL lacks PARP activity (data not shown). (C) Predicted BAL secondary structure and partial homology with KIAA1268. The predicted BAL C-terminal alpha-helical region includes 2 putative short coiled-coil domains (BAL aa 586-617 and aa 746-758) with 4-heptad (BAL aa 586-617) and 2-heptad (BAL aa 746-758) repeats. The BAL aa sequence also displays extended partial homology with a recently described human protein of unknown function, KIAA1268[21] (BAL aa 85-487, 31% identity, 50% homology and BAL aa 160-616, 25% identity, 46% homology, PSI-BLAST). Whereas BAL contains a duplicated N-terminal domain homologous to the nonhistone region of histone macroH2A, the KIAA1268 N-terminus contains 3 repeats of this region. The KIAA1268 C-terminus is also predicted to include an unrelated alpha-helical region with 2 short coiled-coils. (D) Alignment of homologous N-terminal domains of BAL, KIAA1268, and the nonhistone region of histone macroH2A. Identical residues are shown in black and similar residues are shown in gray.

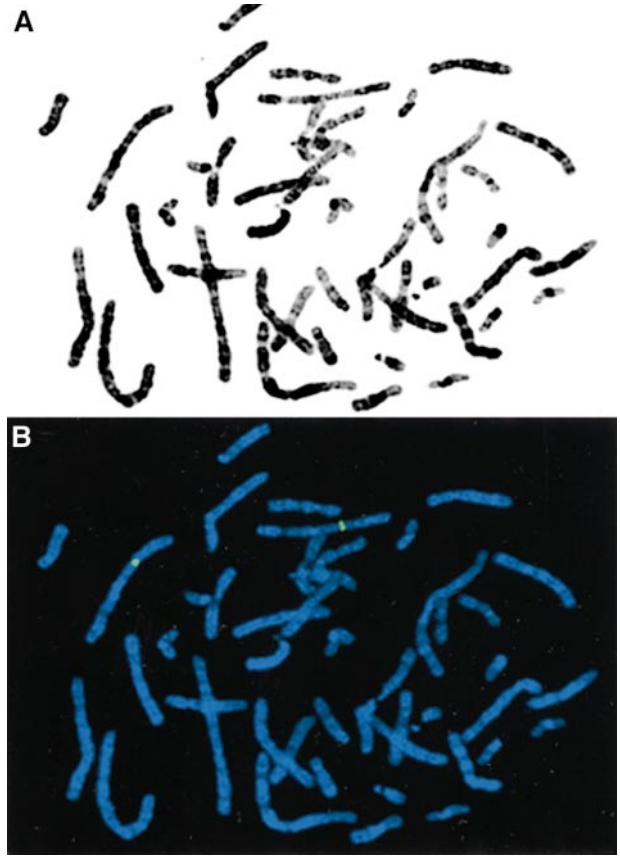

Figure 3. *BAL* chromosomal localization. FISH analysis of a normal human metaphase with genomic PAC clones encompassing the *BAL* locus. (A) Giemsa-banded metaphase. (B) FISH in which the green signals indicate *BAL*-PAC clones hybridized to chromosome band 3q21.

BAL protein expression in B-cell lymphoma cell lines with germinal center or activated peripheral B-cell signatures

Recent microarray analyses suggest that discrete subsets of DLB-CL may derive from GC B cells or activated peripheral blood B cells and that DLB-CL cell lines (such as DHL-6, OCI-Ly3, and OCI-Ly10) express many of the genes that define the distinct GC or activated peripheral B-cell signatures (DHL-6, GC and OCI-Ly3, and OCI-Ly10, activated peripheral B-cell signatures).[7] Similar results were obtained in recent immunophenotypic analyses using a panel of GC and post-GC antigens (F. Wang and M. Shipp, unpublished data, 2000). We have confirmed that DHL-6 and additional DLB-CL cell lines including DHL-4, DHL-7, DHL-8, and DHL-10 express GC antigens (such as CD10 and CD22) whereas the DLB-CL cell lines OCI-Ly3 and OCI-Ly10 express post-GC–activated peripheral B-cell antigens (such as CD44) (data not shown).

To determine whether BAL expression differs in DLB-CL cell lines with GC or activated peripheral B-cell signatures, we evaluated BAL protein levels in the above-mentioned cell lines using an antiserum against the BAL C-terminus (aa 592-854). This antiserum recognized the expected approximately 88 kd BAL protein which was most abundant in DLB-CL cell lines OCI Ly-3, OCI Ly-10, and DHL-7 and less abundant or undetectable in DHL-6, DHL-4, DHL-8, and DHL-10 (Figure 5A).

The fact that BAL is expressed by both cell lines with an activated peripheral B-cell phenotype and only 1 of 5 cell lines with a germinal center signature raises the possibility that BAL expression differs in DLB-CLs derived from unique populations of normal B cells. These observations are of particular interest because these subsets of normal B cells have inherent differences in trafficking potential. In addition, high-risk DLB-CLs typically present as widely-disseminated disease whereas low-risk tumors present as localized nodal disease.[2] For these reasons, we evaluated the effects of BAL on cellular migration.

Functional assessment of BAL B-cell lymphoma transfectants: migration assays

Multiple independent stable *BAL* and vector-only B-cell lymphoma transfectants were generated (see "Materials and methods") for use in cellular migration assays. These pRcCMV-BAL transfectants expressed levels of the BAL protein comparable to those in BAL-positive DLB-CL cell lines whereas vector-only transfectants lacked BAL expression (Figure 5A).

Cellular migration assays were performed using a transwell system in which BAL-positive or vector-only transfectants were plated in the upper transwell chamber. Thereafter, transfectants were evaluated for migration through a separating 8-μm membrane into lower transwell chambers that contained medium alone or medium supplemented with the hematopoietic chemoattractant factor, SDF-1α.[16] In multiple independent assays, the BAL-positive transfectants had approximately 4-fold higher rates of migration than vector-only transfectants ($P < .0001$, Figure 5B). These observations are likely to be relevant to primary DLB-CLs because the levels of BAL protein and transcripts in BAL

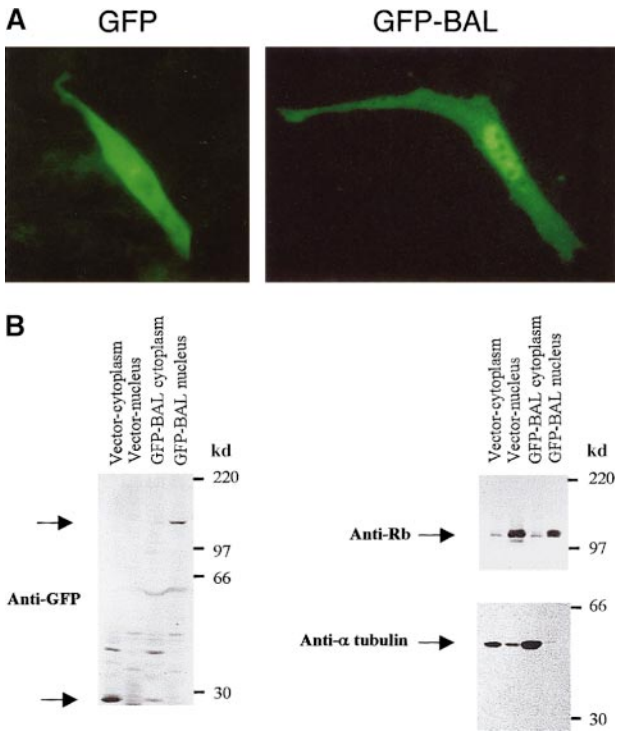

Figure 4. Subcellular localization of the BAL protein. (A) Fluorescence microscopy of NIH3T3 fibroblasts transfected with an expression vector encoding GFP alone (left) or GFP-BAL (right). Whereas fibroblasts transfected with GFP alone exhibit diffuse primarily cytoplasmic GFP (left), cells transfected with GFP-BAL exhibit mainly nuclear fluorescence. (B) Western blot analysis of subcellular fractions from aggressive B-cell lymphoma transfectants expressing either GFP alone or GFP-BAL. Cytoplasmic and nuclear cell fractions were blotted and probed with GFP antiserum (left panel) or control antibodies directed against known cytoplasmic (αtubulin, right lower panel) and nuclear (retinoblastoma [Rb], right upper panel) proteins. In these B-cell transfectants, GFP alone (approximately 26 kd) was primarily detected in the cytoplasm whereas GFP-BAL (approximately 114 kd) was predominantly found in the nucleus.

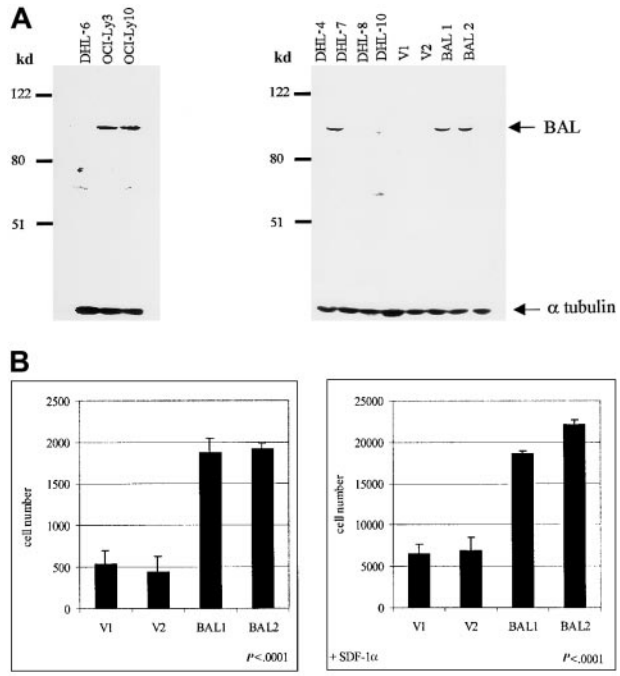

Figure 5. The effects of BAL overexpression on cellular migration. (A) Western blot analysis of BAL expression in aggressive B-cell lymphoma cell lines (DHL-6, OCI-Ly3, OCI-Ly10, DHL-4, DHL-7, DHL-8, and DHL-10) and stable pRcCMV-only or pRcCMV-BAL B-cell lymphoma transfectants. An antiserum generated against the BAL C-terminus recognizes the expected approximately 88 kd BAL protein, which is most abundant in the OCI-Ly3, OCI-Ly10, and DHL-7 cell lines. The BAL antiserum recognizes the expected approximately 88 kd BAL protein in pRcCMV-BAL but not pRcCMV-only transfectants. The blot was also probed with anti-tubulin to confirm equal loading. (B) Transwell migration assays of BAL-overexpressing or vector-only B-cell lymphoma transfectants. Two independent pRcCMV-only and pRcCMV-BAL transfectants were evaluated for migration through a separating 8-μm membrane into lower transwell chambers that contained medium alone or medium supplemented with SDF-1α. The results are represented as the mean number of cells that have migrated to the lower chamber in presence or absence of recombinant human SDF-1α (right and left panels respectively). BAL-overexpressing transfectants had approximately 4-fold higher rates of migration than vector-only transfectants in either the presence or absence of SDF-1α ($P < .0001$, Student 1-sided *t* test).

transfectants, the indicated DLB-CL cell lines, and the high risk primary DLB-CLs are comparable (Figure 1B,D and Figure 5A). BAL increased cellular migration to the same degree in the presence or absence of SDF-1α (Figure 5B, compare left and right panels) indicating that BAL functions independently of the SDF-1α–CXCR-4 pathway or downstream of SDF-1α–CXCR-4 ligation.[16]

Discussion

The newly identified *BAL* gene encodes a protein that is significantly more abundant in high-risk DLB-CLs than in low-risk tumors. BAL overexpression increases the rate of migration of B-cell lymphoma transfectants, suggesting that the risk-related protein may promote the dissemination of high-risk DBL-CLs.

The extensive N-terminal homology between BAL and KIAA1268 suggests that these proteins are encoded by members of a newly identified gene family characterized by variable numbers of highly conserved N-terminal repeats and divergent C-terminal alpha-helical domains. Although the function of the N-terminal repeat in BAL and KIAA1268 is not yet known, this evolutionarily conserved domain has been identified in histone mH2A and certain bacterial and viral proteins.[18] Histone mH2A is preferentially concentrated in the inactive X chromosome of female mammals, prompting speculation that the protein participates in gene inactivation.[24] The cell type–specific and developmentally regulated expression of mH2A further suggest that the protein (and the BAL/KIAA1268–homologous domain) may participate in the establishment and/or maintenance of specific patterns of gene expression.[24] These observations are of additional interest given the increased expression of BAL in DLB-CL cell lines with an activated peripheral B-cell phenotype.

The BAL C-terminus predicts an alpha-helical region with 2 short coiled-coil domains. Although classic long coiled-coils participate in the formation of mechanically rigid structures such as the cytoskeleton, contractile levers, and scaffolding for regulatory complexes, short coiled-coils are found in several families of transcriptional regulators.[25] In these proteins, the short coiled-coil domains mediate combinatorial rearrangements that position DNA-binding regions on the DNA.[25] A series of DNA and RNA processing enzymes also include short coiled-coil domains that form the mechanical tools for gripping, guiding, or moving substrates during the reaction cycle.[25] Given the nuclear localization of BAL, it is possible that its short coiled-coil domains and histone macro2A-homologous N-terminal repeats function to modulate gene expression and, consequently, regulate pathways implicated in cellular migration.

The localization of BAL and KIAA1268 to chromosome 3q21 is of particular interest because 3q21 is an area of known abnormalities in multiple hematologic malignancies. Amplifications, translocations, and additional less common abnormalities of 3q21 have been described in B-cell tumors including DLB-CL, mantle cell lymphoma, and marginal zone lymphoma.[26-32] The identification of large genomic clones that encompass the *BAL* locus will make it possible to use FISH to analyze B-cell lymphomas with 3q21 abnormalities for *BAL* disruption. Although 3q21 abnormalities may contribute to dysregulated BAL expression in certain B-cell neoplasms, the common and consistent risk-related differences in BAL expression in DLB-CLs are likely to have additional explanations.

It is possible that BAL expression is developmentally regulated during normal B-cell differentiation and that DLB-CLs derived from discrete populations of normal B cells have inherent differences in BAL expression and trafficking potential. The increased expression of BAL in DLB-CL cell lines with an activated peripheral B-cell phenotype is consistent with this hypothesis. In an initial report, patients whose DLB-CLs had an activated peripheral B-cell phenotype had poorer outcomes than patients whose tumors had a GC B-cell signature.[7] However, in this study, cell of origin–associated differences in outcome were most striking among patients with IPI-defined low/low-intermediate risk disease (L/LI)[7] (also L. Staudt, personal communication, March 2000). In high-risk tumors, differences in tumor microenvironment or relevant signaling pathways may also modulate BAL expression. Once BAL monoclonal antibodies that work on paraffin-embedded tissues are available, we will be able to evaluate the relationship between BAL expression, specific clinical risk factors (such as stage), and putative cell of origin in an expanded series of primary DLB-CLs. Further insights into the regulation and function of the risk-related *BAL* gene and associated family members will increase our understanding of the heterogeneity and pathogenesis of DLB-CLs and, possibly, lead to the identification of novel therapeutic targets.

Acknowledgments

We thank I. Grogan and G. Pinkus for assistance in identifying appropriate primary DLB-CLs for further analysis.

References

1. Shipp M, Harris N, Mauch P. The non-Hodgkin's lymphomas. In: DeVita VT, Hellman S, Rosenberg SA, eds. Cancer Principles & Practices of Oncology. Philadelphia, PA: J.B. Lippincott; 1997: 2165-2220.
2. Shipp M, Harrington D, Chairpersons, Anderson J, Armitage J, Bonadonna G, et al. A predictive model for aggressive non-Hodgkin's lymphoma: the International NHL Prognostic Factors Project. N Engl J Med. 1993;329:987-994.
3. Kuppers R, Klein U, Hansmann M-L, Rajewsky K. Cellular origin or human B-cell lymphomas. N Engl J Med. 1999;341:1520-1529.
4. Drillenburg P, Pals S. Cell adhesion receptors in lymphoma dissemination. Blood. 2000;95:1900-1910.
5. Cyster J. Chemokines and cell migration in secondary lymphoid organs. Science. 1999;286: 2098-2102.
6. Bleul C, Schultze J, Springer T. B lymphocyte chemotaxis regulated in association with microanatomic localization, differentiation state, and B cell receptor engagement. J Exp Med. 1998;187: 753-762.
7. Allzadeh A, Elsen M, Davis R, et al. Distinct types of diffuse large B-cell lymphoma identified by gene expression profiling. Nature. 2000;4051: 503-511.
8. Kulidjian A, Inman R, Issekutz T. Rodent models of lymphocyte migration. Sem in Immunol. 1999; 11:85-93.
9. Lauffenburger D, Horwitz A. Cell migration: a physically integrated molecular process. Cell. 1996;84:359-369.
10. Tsuzuki S, Toyama-Sorimachi N, Kitamura F, et al. Intracellular signal-transducing elements involved in transendothelial migration of lymphoid cells. Jpn J Cancer Res. 1998;89:571-577.
11. Aguiar R, Yakushijin Y, Kharbanda S, Tiwari S, Freeman G, Shipp M. PTPROt: an alternatively spliced and developmentally regulated B-lymphoid phosphatase that promotes GO/G1 arrest. Blood. 1999;94:2403-2413.
12. Liang P, Pardee A. Differential display of eukaryotic messenger RNA by means of polymerase chain reaction. Science. 1992;257:967.
13. Xiao S, Nalabolu S, Aster J, et al. FGFR1 is fused with a novel zinc-finger gene, ZNF198, in the t(8;13) leukaemia/lymphoma syndrome. Nat Gen. 1998;18:84-87.
14. Aguiar R, Sohal J, Van Rhee F, et al. TEL-AML1 fusion in acute lymphoblastic leukemia of adults. Br J Haematol. 1996;95:673-677.
15. Duan D, Humphrey J, Chen D, et al. Characterization of the VHL tumor suppressor gene product: localization, complex formation, and the effect of natural inactivating mutations. Proc Natl Acad Sci U S A. 1995;92:6459-6463.
16. Bleul C, Fuhlbrigge R, Casasnovas J, Aiuti A, Springer T. A highly efficacious lymphocyte chemoattractant, stromal cell-derived factor 1 (SDF-1). J Exp Med. 1996;184:1101-1109.
17. Pehrson J, Fried V. MacroH2A, a core histone containing a large nonhistone region. Science. 1992;257:1398-1400.
18. Pehrson J, Fuji R. Evolutionary conservation of histone macroH2A subtypes and domains. Nucleic Acids Res. 1998;26:2837-2842.
19. Lupas A. Predicting coiled-coil regions in proteins. Curr Opin Struct Biol. 1997;7:388-393.
20. Ren R, Mayer B, Cicchetti P, Baltimore D. Identification of a ten-amino acid proline-rich SH3 binding site. Science. 1993;259:1157-1161.
21. Nagase T, Ishikawa K, Kikuno R, Hirosawa M, Nomura N, Ohara O. Prediction of the coding sequences of unidentified human genes, XV: the complete sequences of 100 new cDNA clones from brain which code for large proteins in vitro. DNA Res. 1999;6:337-345.
22. Ohno S: Gene duplication and the uniqueness of vertebrate genomes circa 1970-1999. Semin Cell Dev Biol. 1999;5:517-522.
23. Smith N, Knight R, Hurst L. Vertebrate genome evolution: a slow shuffle or a big bang? Bioassays. 1999;8:697-703.
24. Costanzi C, Pehrson J. Histone macroH2A1 is concentrated in the inactive X chromosome of female mammals. Nature. 1998;393:599-601.
25. Lupas A. Coiled coils: new structures and new functions. Trends Biochem Sci. 1996;21:375-382.
26. Mitelman F, Mertens F, Johansson B. A breakpoint map of recurrent chromosomal rearrangements in human neoplasia. Nat Genet. 1997; 15(special no.):417-474.
27. Monni O, Oinonen R, Elonen E, et al. Gain of 3q and deletion of 11q22 are frequent aberrations in mantle cell lymphoma. Genes Chromosomes Cancer. 1998;21:298-307.
28. Schlegelberger B, Zwingers T, Harder L, et al. Clinicopathogenetic significance of chromosomal abnormalities in patients with blastic peripheral B-cell lymphoma. Blood. 1999;94:3114-3120.
29. Cigudosa J, Parsa N, Louie D, et al. Cytogenetic analysis of 363 consecutively ascertained diffuse large B-cell lymphomas. Genes Chromosomes Cancer. 1999;25:123-133.
30. Khokhar M, Brito-Babapulle V, Matutes E, Catovsky D. Cytogenetic abnormalities in the leukemic phase of non-Hodgkin's lymphoma. Cancer Genet Cytogenet. 1995;83:18-24.
31. Schouten H, Sanger W, Weisenburger D, Anderson J, Armitage J. Chromosomal abnormalities in untreated patients with non-Hodgkin's lymphoma: associations with histology, clinical characteristics, and treatment outcome. The Nebraska Lymphoma Study Group. Blood. 1990;75:1841-1847.
32. Cabanillas F, Pathak S, Trujillo J, et al. Frequent nonrandom chromosome abnormalities in 27 patients with untreated large cell lymphoma and immunoblastic lymphoma. Cancer Res. 1988;48: 5557-5564.
33. Smith S, Giriat I, Schmitt A, de Lange T. Tankyrase, a poly(ADP-ribose) polymerase at human telomeres. Science. 1998;282:1484-1487.